This is an Accepted Manuscript of a conference paper published by Taylor & Francis in [24th Australasian Conference on the Mechanics of Structures and Materials, 6-9 Dec 2016, Perth, Australia]" ***Please cite:*** *Nakamura, Y., Derakhshan, H., Sheikh, H., Griffith, M., Ingham, J. (2016) Investigation of equivalent frame modelling for seismic analysis of unreinforced masonry building with flexible diaphragms. 24th Australasian Conference on the Mechanics of Structures and Materials, 6-9 Dec 2016, Perth, Australia.*

Investigation of equivalent frame modelling for seismic analysis of unreinforced masonry buildings with flexible diaphragms

Y. Nakamura, H. Derakhshan, H. Sheikh & M.C. Griffith
University of Adelaide, Australia

J. Ingham
University of Auckland, New Zealand

ABSTRACT: A case study was conducted to investigate the applicability of equivalent frame modelling for the nonlinear time-history analysis of unreinforced masonry buildings with flexible diaphragms. The dynamic responses calculated from the equivalent frame models were compared against shake table test results of a full-scale two-storey stone masonry building. The investigated modelling approach reflected the simplifications commonly assumed for the global analysis of buildings; namely, considering the diaphragms to behave elastically and neglecting the stiffness and strength contributions of the out-of-plane responding walls. The sensitivity of the analysis to different idealisations of the equivalent frame and diaphragm stiffness values were also investigated. Discussions are provided on the accuracies and limitations of the investigated modelling approach, which may serve as a useful guidance for practical application.

1 INTRODUCTION

Unreinforced masonry (URM) buildings make up a substantial proportion of existing building stock, and continue to pose large seismic risk in many parts of the world. In evaluating their seismic vulnerability, efficient numerical models are required, that are capable of simulating the inelastic building behaviour. The equivalent frame modelling procedure (Magenes & Della Fontana 1998) has been shown to be a promising practical approach capable of simulating the salient response mechanisms of URM buildings, without incurring the large computational penalty of finite element analysis.

The equivalent frame idealisation considers the in-plane response of a wall as comprising of deformable pier and spandrel elements connected to nodes, which may have rigid offsets (Fig. 1(a)). The minimum deformable length of the piers (spandrels) is commonly assumed to be dictated by the smallest height (width) of adjacent openings. Alternatively, to account for the deformability of the node panels, the deformable length of piers may be extended (for example, making use of 30° lines emanating from the corners of the door or window openings) as shown in Figure 1(a). The piers and spandrels are conceptually represented as elastic frame members with lumped nonlinearity capturing the shear or rocking failure modes (Fig.1(b)).

The two-dimensional equivalent frames can be used to simulate the global three-dimensional responses of buildings, by assembling the equivalent frames connected at the floor levels by diaphragms (Lagomarsino et al. 2013). In such three-dimensional models, floor and roof diaphragms are often treated as stiffness contributing elements but do not have dynamic or vibration characteristics.

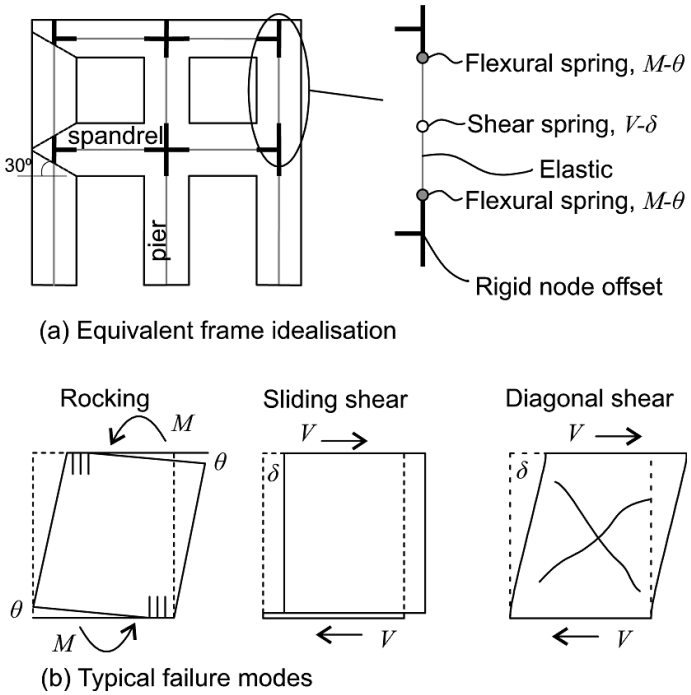

Figure 1: Equivalent frame idealisation and typical failure modes

However, it is well recognised that the in-plane motions of flexible timber diaphragms can dominate the response of these buildings. Despite the importance of the dynamic characteristics of flexible diaphragms, the accuracy of an equivalent frame analysis incorporating such behaviour has not been investigated in detail so far. The aim of this paper is to explore the applicability of the equivalent frame modelling approach for the prediction of the global response of URM buildings with flexible diaphragms, considering various modelling limitations currently faced by practising engineers. To this end, a relatively simple numerical model based on commonly accepted assumptions is investigated. Specifically, the diaphragms are represented by elastic membrane elements, while the out-of-plane wall stiffness and strength contributions are neglected. Dynamic test data of a full-scale stone masonry building with strengthened timber floor and roof (Magenes et al. 2014) is used to verify the potential, and to identify the limitations, of the simplified modelling approach. While the analyses are conducted using TREMURI (Lagomarsino et al. 2013) with certain modelling concepts specific to that program, results reported in this paper have general applicability.

2 CASE STUDY BUILDING

A two-storey stone masonry building with a timber floor and a timber roof diaphragm tested at EUCENTRE (Magenes et al. 2014) was analysed in this study. This is a retrofitted building (Fig. 2), whose diaphragms had been strengthened with a layer of diagonal timber boards nailed to the original single straight sheathing. The connections between the floor/roof diaphragms and the walls were also strengthened by steel ring beams at the floor level, and a continuous reinforced masonry ring beam at the roof level. These strengthening measures ensured the global building behaviour to take place, while still allowing some level of diaphragm flexibility.

The building was tested under shake table excitations using the motions of the 15 April 1979 Montenegro earthquake measured at the Ulcinj-Hotel Albatros station. The nominal peak ground acceleration (PGA) was gradually increased from 0.05g to 0.7g, for which the actual acceleration (peak) of the table motion varied from 0.06g to 1.16g. In this paper, the excitation levels are referred to by the nominal PGA. The response of the building was almost elastic up until the 0.5g excitation. Significant cracking appeared during the 0.6g test sequence, followed by the near-collapse state with the 0.7g excitation. A detailed description of the response characteristics of the building can be found in (Magenes et al. 2014).

3 MODELLING APPROACH

3.1 *General Description*

In equivalent frame modelling, each wall is idealised as equivalent plane (2D) frame members consisting of piers and spandrels. These members are connected to nodes at their two ends, with each node having in-plane local degrees of freedom. Three-dimension nodes (3D wall nodes) are used at the intersections of walls to model box-type behavior. However, the contributions of out-of-plane stiffness and strength of a wall that are usually small compared to its in-plane stiffness and strength are neglected. The compatibility of the two intersecting walls is strictly satisfied for the vertical translation, but not for the horizontal translational or the rotational components. This modelling concept allows the direct adoption of the 2D equivalent frame idealisation developed for the individual walls in isolation. In this way, flange effects at wall intersections associated to normal deformations are captured in an approximate manner, allowing free warping of the flanged section, whereas no flange effect is captured for shear deformation.

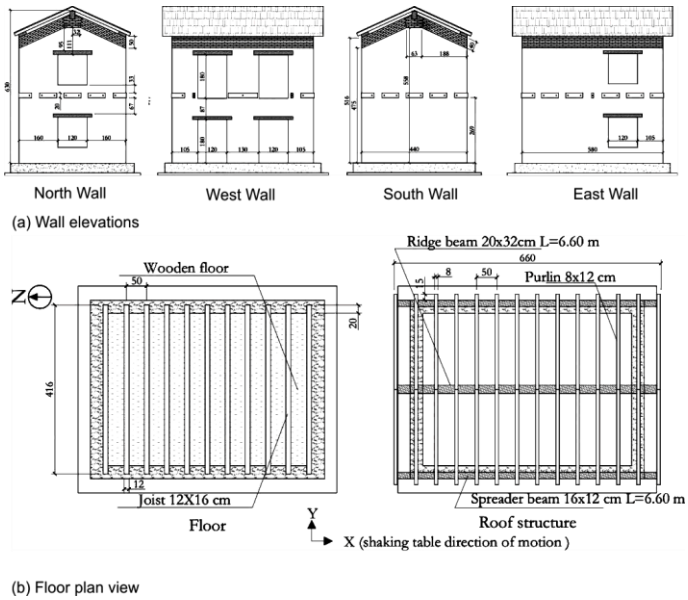

Figure 2: Construction details of tested building, dimensions in cm (Magenes et al. 2014)

The diaphragms are modelled with plane stress or membrane elastic elements where the element node (2D diaphragm node) consists of two in-plane (horizontal) translational degrees of freedom, which permit a linear variation of displacements within an element. These elements are defined by the Young's modulus, shear modulus, and the thickness of the diaphragms. In this study, four elements are used to model a single diaphragm, which is the simplest possible idealisation that can capture the vibration characteristics of the diaphragms.

The nodal masses are assigned by considering simple tributary areas for inertial (horizontal) loads, (Fig. 3). It should be noted that distributing the mass in this manner does not provide the correct internal force distribution under gravity loading. Thus, additional static nodal forces (vertical forces and moments) are applied in order to obtain the correct gravity forces prior to the dynamic analysis.

3.2 *Macroelement properties*

The inelastic behaviours of the piers and spandrels are simulated using the macroelement definition of TREMURI (Penna et al. 2014). The macroelement captures the axial-rocking behaviour accounting for the limited compressive capacity and the stiffness and strength degradations under shear deformation, as governed by an internal damage parameter. The material properties used in the present analyses (Table 1) were obtained from the results of complementary component tests as part of the experimental campaign (Magenes et al. 2010).

Table 1: Masonry material properties from component tests

Young's modulus (MPa)	Shear modulus (MPa)	Compressive strength f_m (MPa)	Cohesion f_{v0} (MPa)	Friction coefficient μ
2537	841	3.28	0.14	0.14

3.3 *Analysis cases*

In order to explore uncertainties associated with the choice of modelling, four different analysis cases were considered. These cases corresponded to two different idealisations of the equivalent frame definitions, and diaphragm stiffness values calculated using two different approaches.

The two equivalent frame idealisations of the walls oriented in the direction of loading are shown in Figure 4. The first idealisation corresponds to the "full" rigid offsets of the nodes where the rigid zones extend across the full width or the depth of pier and spandrel. The second pattern reflects the actual crack patterns of the tested building, capturing both the initial damage suffered during the transportation of the building as well as the crack pattern observed from the final stage of testing (reported in a subsequent section of this paper).

In addition to the equivalent frame idealisations, two sets of diaphragm stiffness values were considered. The first values (D1) corresponded to the expected diaphragm stiffness suggested by ASCE 41-13 (ASCE 2014). The second stiffness values (D2) were calculated more rigorously using the procedure proposed by Brignola et al. (2012), by considering the timber joists to act as flexural beams in parallel. In the latter approach, the interior joists were assumed to be pinned at wall connections, while the end joists were fixed, with the fixity provided by the perimeter ring beams.

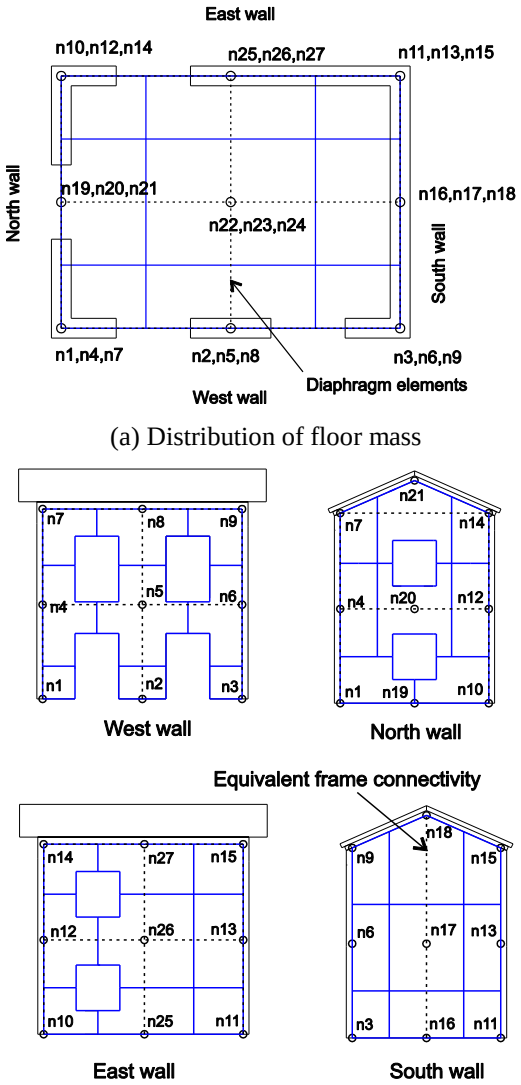

(a) Distribution of floor mass

(b) Distribution of wall mass

Figure 3: Tributary areas for the distribution of the mass

In addition, the steel beam and the uncracked portion of the masonry wall, as observed from the final test run, were also considered to provide additional stiffness for the floor diaphragm. For the roof diaphragm, the perimeter reinforced masonry beam was included in the stiffness calculation.

The four models analysed were:

- Case 1: full rigid offset with D1
- Case 2: full rigid offset with D2
- Case 3: cracked pattern with D1
- Case 4: cracked pattern with D2

4 ANALYSIS OF RESULTS AND DISCUSSION

The accuracies of the numerical models were studied by comparing the predicted results against the

experimental data in terms of the modal properties and peak displacements.

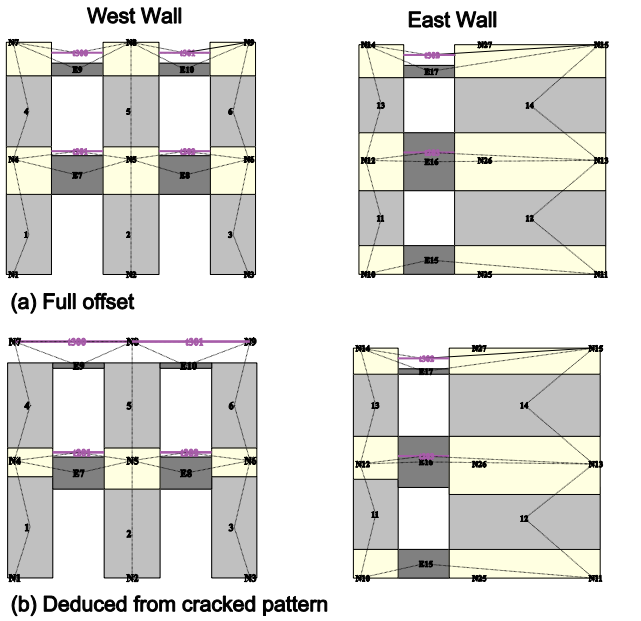

Figure 4: Equivalent frame idealisation of longitudinal walls

The modal properties are presented in Figure 5 and Figure 6 for the experiment and numerical results respectively. The same number of significant modes in the direction of excitation were identified from the experimental results and the numerical analysis. The fundamental mode of vibration in the direction of excitation is reasonably well captured by all analysis models. It can be seen that the increase in the displacement value up the height of the building is better captured when the diaphragm stiffnesses are calculated using the more refined procedure (Cases 2 and 4). In particular, the closest fundamental mode shape is achieved by Case 4. In general, the numerical models exhibit larger deformations of the diaphragms relative to the walls, and underestimate the fundamental frequency in comparison to the experimental result.

In contrast to the fundamental mode, the higher modes are not captured so well. The out-of-phase vibration of the floor and the roof diaphragms is more pronounced in the numerical analysis compared to that observed experimentally (2nd significant mode). The 3rd experimentally observed mode resembling the rotation of the diaphragms as a rigid-body could not be identified by the numerical models. The highest significant mode shape found in the experiment appears to be a mixture of the two highest modes predicted by the numerical models.

The larger diaphragm displacements and the reduced torsional rotation are due to the lack of coupling between the diaphragms at adjacent levels, as well as a lack of coupling between diaphragms and the in-plane loaded walls. This coupling is provided by the out-of-plane deformations of walls, which were neglected in the analysis. The implication is that the out-of-plane walls may play an important role (particularly if the height-to-thickness ratio of the wall is not large, as in the tested building), at least within the elastic range of the building response.

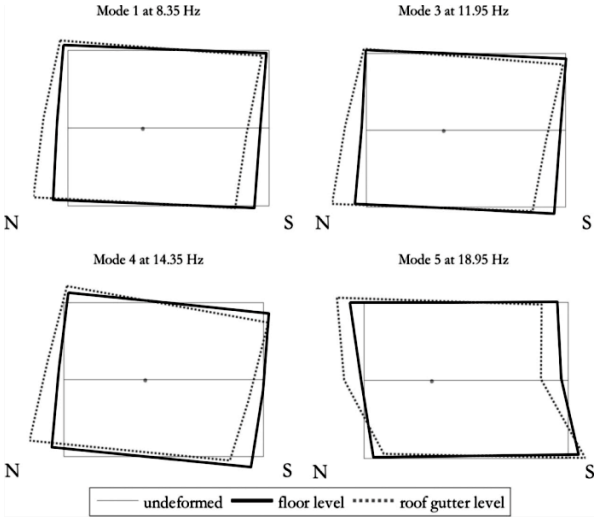

Figure 5: Mode shapes and frequencies identified from ambient and random vibrations (Magenes et al. 2014)

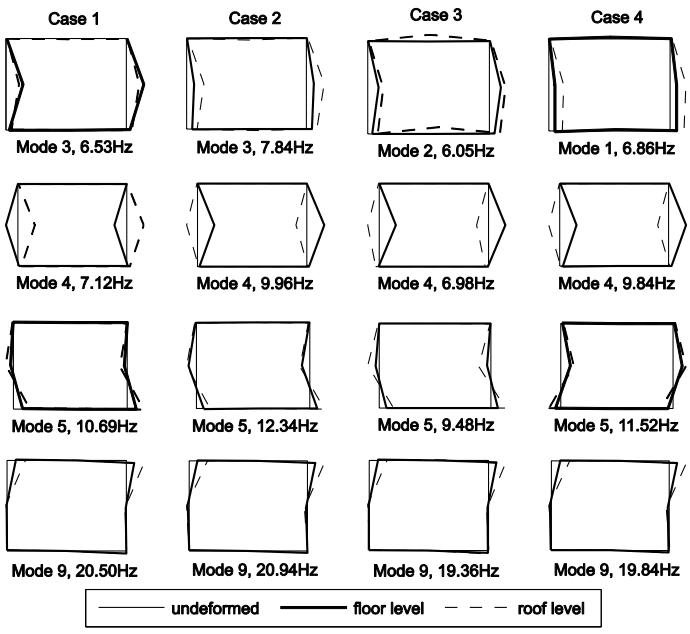

Figure 6: Significant mode shapes and frequencies from numerical analysis

The peak displacement envelopes found experimentally, as well as numerically, are compared in Figure 7 for the West and East walls as well as at the diaphragm mid-spans. The results corresponding to 0.4g, 0.5g, 0.6g and 0.7g excitation intensities are shown for the four analysis cases. The general trends of the experimental results show that the peak displacements of the walls and the diaphragms approach towards each other as the excitation intensity increases. This trend is captured by all numerical models also. In general, the sensitivity of the analysis to the diaphragm stiffness is small, although the elastic response (0.4g and 0.5g intensities) is affected to some degree. The discretisation of the equiva-

lent frame appears to have more importance. The upper storey displacements of the West wall are better captured by Cases 3 and 4 in the elastic range, implying that the equivalent frame idealisation based on the cracked pattern provides a better correlation with the experimental data. However, when significant inelastic response occurs during the 0.7g excitations, no significant differences of these responses predicted by the four different models are found, and all models underestimate the upper storey deformation.

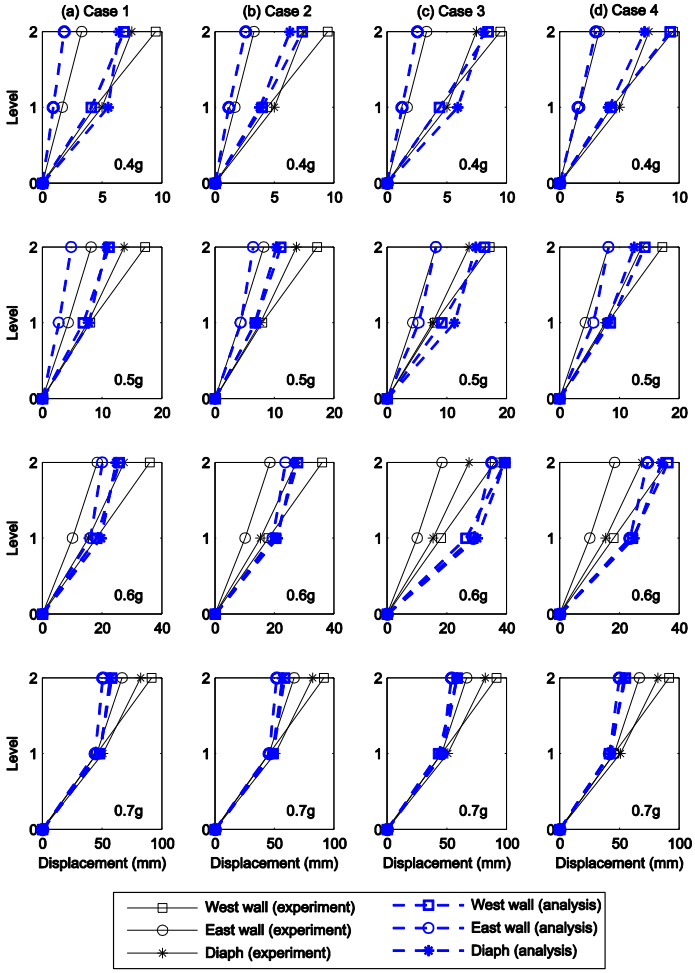

Figure 7: Comparisons of peak displacement envelopes

5 INFLUENCE OF DIAPHRAGM FLEXIBILITY

The sensitivity of the building response due to relatively large diaphragm flexibility was investigated numerically. Using the analysis Case 4, the stiffnesses of the floor and the roof diaphragms were reduced from their original values (D2) to 0.005 times the original values. Figure 8(a) shows the peak displacement variations of the West and the East walls at the roof level (u^r_{west} and u^r_{east} respectively) as well as the peak deformation of the roof diaphragm mid-span relative to the walls (Δ^r_d). The results correspond to the 0.6g excitation, and are plotted against the average diaphragm period (T_d) of the floor and the roof. The diaphragm periods approximately corresponding to the diaphragm stiffness D1 (Table 2) and the lower-bound stiffness suggested by ASCE 41-13 (ASCE 2014) are also indicated. It can be observed that the diaphragm flexibility has significant effects on the seismic demands of the in-plane response of walls. In particular, for the West wall, which is more flexible, a displacement amplification of 220% is observed between the as-built diaphragm D2 and the lower-bound values.

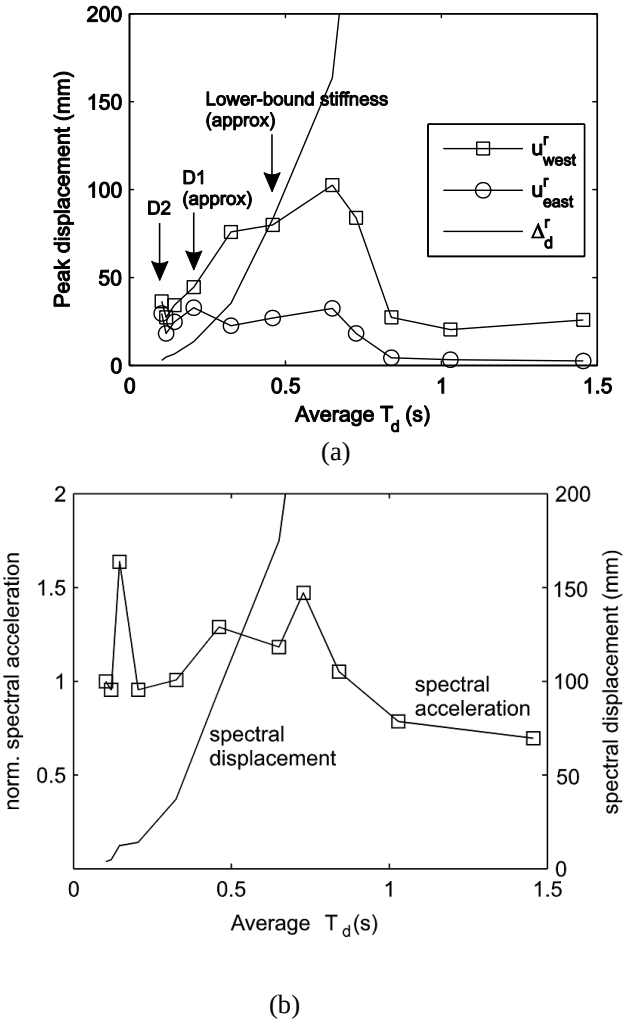

Figure 8: (a) Effect of diaphragm flexibility on wall displacement and roof deformation; (b) normalised spectral acceleration and displacement, plotted against the average diaphragm period T_d subjected to the 0.6 g excitation.

Such amplification is due to two factors associated with flexible diaphragms; namely, (1) the variation of the diaphragms' inertial forces and (2) reduced coupling between the walls when the diaphragm are flexible. The effect of the first factor can be seen in Figure 8(b), where the spectral acceleration of the 0.6g table motion is plotted with respect to the diaphragm periods (normalised with respect to values corresponding to the original diaphragm). The comparison between the spectral accelerations and the peak wall displacements indicates that the wall displacement amplifications occur when the spectral accelerations (or inertial forces) of the diaphragms are amplified. Once the spectral acceleration is re-

duced for T_d greater than approximately 0.7 s, the peak wall displacement is also reduced. The peak inertial force of the diaphragm hence directly affects the displacement demands of the walls. This observation also implies that the amplification is dependent on the ground motion characteristics. The second factor exacerbates the amplification of the weaker/flexible side (i.e. West wall) due to the limited coupling provided by flexible diaphragms in redistributing the internal forces.

It can also be seen that the peak diaphragm deformation (Fig. 8(a)) closely reflects the spectral displacement (Fig. 8(b)), suggesting that the diaphragm deformation may be estimated directly from the elastic spectrum.

However, it is questionable if the diaphragm deformation actually matches the spectral displacement when the diaphragm is overly flexible, without causing instability of the out-of-plane responding walls. Further studies are needed to investigate the effect of the dynamic response of the out-of-plane walls (particularly for the two-way spaning walls) on the building response when the diaphragm becomes excessively flexible.

6 CONCLUSIONS

In this paper, results of a case study are reported on the applicability of the equivalent frame modelling approach for URM buildings with flexible diaphragms. Reflecting the current modelling practice, the diaphragms were considered to remain elastic and the out-of-plane wall stiffness and strength contributions were neglected.

The simple modelling approach was able to capture, with reasonable accuracy, the fundamental mode characteristics and the evolution of the peak displacements as the excitation intensity increased. On the other hand, the higher modes were not as accurately simulated.

More consistent displacement predictions were achieved when the equivalent frame idealisation reflected the actual crack pattern.

For the case study building, the analyses did not indicate large sensitivity to the diaphragm stiffness values. When the diaphragms were made relatively flexible, however, the numerical models indicated the potential for significant sensitivity, including amplification, of the wall displacements due to the diaphragm stiffness values.

The analyses also revealed that perhaps the most significant limitation of the investigated modelling approach is the omission of the out-of-plane walls. The discrepancies in the mode properties were identified as primarily due to the lack of out-of-plane wall stiffness. The interaction between the out-of-plane responding wall and flexible diaphragm is also expected to play an important role as the diaphragm flexibility increases. In such cases, a numerical modelling approach capable of simulating the two-way spanning out-of-plane walls, including finite element modelling, may be preferred.

7 ACKNOWLEDGEMENTS

This work was supported by the Australian Research Council, through the grant DP120100848. The first author received financial support through the Australian Postgraduate Award. The authors would like to thank Prof. Magenes, Asst. Prof. Penna and Dr. Senaldi from the University of Pavia and EUCENTRE for their suggestions on the numerical modelling of the experimentally tested building. The authors would also like to thank Prof. Magenes for reviewing the original manuscript.

8 REFERENCES

ASCE 2014. *Seismic evaluation and retrofit of existing buildings ASCE/SEI 41-13.* American Society of Civil Engineers, Reston, Virginia.

Bringola A., Pampanin S., Podesta S. 2012. Experimental evaluation of the in-plane stiffness of timber diaphragms. *Earthquake Spectra*. 28(4). 1687 - 1709.

Kappos A.J., Penelis G.G., Drakopoulos C.G. 2002. Evaluation of simplified models for lateral load analysis of unreinforced masonry buildings. *Journal of Structural Engineering*. 128(7). 890 – 897.

Lagomarsino S., Penna A., Galasco A., Cattari S. 2013. TREMURI program: An equivalent frame model for the nonlinear seismic analysis of masonry buildings. *Engineering Structures*. 56. 1787 - 1799.

Magenes G., Della Fontana A. 1998. Simplified non-linear seismic analysis of masonry buildings. *Proc. of the British Masonry Society*. 8. 190 – 195.

Magenes G., Penna A., Galasco A., Da Paré M. 2010. In-plane cyclic shear tests of undressed double-leaf stone masonry panels. *Proc. of 8th International Masonry Conference*, Dresden.

Magenes G., Penna A., Senaldi I., Rota M., Galasco A. 2014. Shaking table test of a strengthened full-scale stone masonry building with flexible diaphragms. *International Journal of Architectural Heritage: Conservation, analysis and restoration*. 8(3). 349 - 375.

Penna A., Lagomarsino S., Galasco A. 2014. A nonlinear macroelement model for the seismic analysis of masonry buidlings. *Earthquake Engineering and Structural Dynamics*. 43(2). 159 - 179.

Salonikios T., Karakostas C., Lekidis V., Anthoine A. 2003. Comparative inelastic pushover analysis of masonry frames. *Engineering Structures*. 25. 1515 – 1523.